Hydrogen evolution, incorporation and removal in electroless nickel composite coatings on aluminium

I. APACHITEI* and J. DUSZCZYK

Laboratory of Materials Science, Delft University of Technology, Rotterdamseweg 137, 2628 AL Delft, The Netherlands

(*author for correspondence, e-mail: i.apachitei@stm.tudelft.nl; fax: +31 15 2786730)

Abstract

The mechanism of electroless nickel deposition involves generation of hydrogen which can be entrapped in the NiP layer. In this study hydrogen evolution in several electroless composite coatings, that is, NiP–X (X = SiC, Al_2O_3 and boron particles), deposited on an aluminium (6063-T6) substrate, was investigated by the solid extraction method. It was found that particle codeposition can promote hydrogen occlusion in the layers, a fact correlated with the adsorption capacity and affinity of particles towards water or hydrogen itself. Hydrogen removal efficiency from coatings, after heat treatment, increased with the applied temperature (130, 160 and 190 °C for 1.5 h each). For the same heat treatment (190 °C for 1.5 h), most composite coatings showed lower removal efficiencies (35–54%) compared to NiP layer (80%) and, as the amount of hydrogen in the composite coating increased, its removal efficiency decreased.

1. Introduction

Electroless (autocatalytic) deposition from aqueous solution is a reliable method for the production of metal matrix composite coatings. The codeposition of ceramic or solid lubricant particles in a NiP matrix via electroless deposition can produce coatings with high wear resistance or self-lubricating properties, correlated with an excellent layer uniformity and good dimensional accuracy, regardless substrate geometry.

Usually, the presence of hydrogen in metals and alloys induces damage owing to the diffusion of atomic hydrogen in the bulk material, mainly when these are in internal stress. In the literature, this phenomenon is called 'hydrogen embrittlement' and is, in general, associated with a loss in metal or alloy ductility [1]. The response of metals and alloys to hydrogen absorption is different. For example, less than 1 ppm hydrogen content can be sufficient to cause hydrogen embrittlement in high strength steel while in titanium this effect appears only above several hundreds ppm hydrogen [2, 3].

In electroless metal deposition, the electrons required for the reduction of metal ions are supplied through the catalytic oxidation of a reducing agent. A necessary condition for electroless deposition to occur is that the redox potential of the reducing agent (E_R°) has to be more negative than that of the coating metal (E_M°) [4]. Thus, when sodium hypophosphite is used to produce deposits from a solution containing nickel ions, the $E_R^\circ = -0.50$ V compared to $E_M^\circ = -0.257$ V (against the standard hydrogen electrode) [4, 5]. A consequence of the reactions which take place in the bath is the inevitably generation of hydrogen [6–9].

When a metal substrate is subjected to a finishing process by electroless deposition, a certain amount of hydrogen evolved during the process will be trapped in the coating increasing its brittleness. On the other hand, as was found by Szasz et al. [10], hydrogen may partially take over the role of metalloid stabilizing the amorphous structure of the layer. Since hydrogen has the smallest and lightest atom, it is expected to have a high mobility and to easily diffuse throughout the coated material (e.g., jump frequency at 300 K in α-iron is 10^{12} s^{-1} [11]). As a result, it can negatively affect the adhesion between coating and substrate in the as-deposited state, or even the properties of the substrate itself.

Before electroless plating, metals and alloys undergo a cleaning and/or activation treatment to gain the necessary adhesion for coating. For aluminium and its alloys the most familiar pretreatment includes chemical cleaning followed by a zincating (often double zincating) step. Before and during zincating hydrogen is also released.

This study was aimed to investigate hydrogen incorporation in NiP–X (X = SiC, Al_2O_3 and boron particles) coatings obtained by electroless deposition on aluminium. In addition, hydrogen removal after coatings heat treatment was assessed. Hydrogen content was determined using the solid extraction method. To the authors' knowledge, these results represent the first findings of hydrogen pick-up in electroless NiP composite coatings.

2. Hydrogen occurrence in aluminium substrate

The presence of hydrogen in the aluminium substrate might be attributed to the existent hydrogen in the native substrate and hydrogen introduced by the pretreatment required for electroless nickel deposition.

2.1. Native substrate

Hydrogen represents about 70 to 90% of the total gas content in aluminium alloys [12]. Water vapour reacts with aluminium to form aluminium oxide and hydrogen, this representing the main source of hydrogen in these alloys. The reaction can be written as

$$2\,Al + 3\,H_2O \rightarrow Al_2O_3 + 3\,H_2 \uparrow \qquad (1)$$
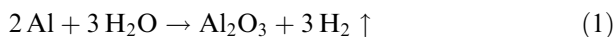
At the freezing point, hydrogen has a 20 times lower solubility in solid aluminium state compared to that in liquid aluminium (0.035 vs 0.7 ppm) [13, 14]. As a consequence, gas porosity can appear during solidification.

Hydrogen is dissolved interstitially in the aluminium lattice. The presence of certain impurities, such as sulphur compounds can also retain hydrogen while some alloying elements, like copper and silicon, decrease the hydrogen uptake [15]. In practice, during the production process, hydrogen from aluminium alloys cannot be completely removed, but only reduced to tolerable limits by degassing.
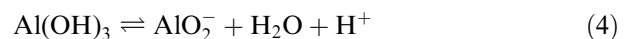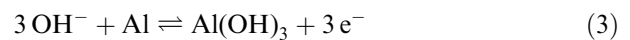
2.2. Aluminium pretreatment

Usually, pure aluminium, and most of its alloys, are catalysts for electroless nickel deposition and can be plated after simple cleaning. Owing to its affinity for

oxygen, aluminium spontaneously forms a thin amorphous Al_2O_3 layer ($\sim 2 - 4$nm [16]) when in contact with air or water (Reaction 1). To secure good adhesion of electroless NiP layer on aluminium substrates, the aluminium oxide layer is removed by a suitable pretreatment sequence. A double immersion zincating process is mostly used [17–20]. During the pretreatment steps, the substrate is immersed in several cleaning solutions when hydrogen evolution occurs. The three main steps in which hydrogen is generated are etching, zincating and stripping. If the etching process takes place in sodium hydroxide solution, the overall reaction is [21]

$$2\,Al + 6\,H_2O \rightleftharpoons 2\,Al\,(OH)_3 + 3\,H_2 \uparrow \qquad (2)$$
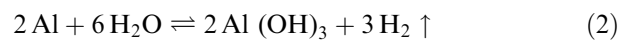
The alkaline zinc immersion process for aluminium substrates can be described as an electrochemical process, occurring by the following reactions [18, 19]:
Dissolution of aluminium (anodic sites)

$$3\,OH^- + Al \rightleftharpoons Al(OH)_3 + 3\,e^- \qquad (3)$$

$$Al(OH)_3 \rightleftharpoons AlO_2^- + H_2O + H^+ \qquad (4)$$

Deposition of zinc (cathodic sites)

$$Zn(OH)_4^{2-} \rightleftharpoons Zn^{2+} + 4\,OH^- \qquad (5)$$

$$Zn^{2+} + 2\,e^- \rightleftharpoons Zn^0 \qquad (6)$$

$$H^+ + e^- \rightleftharpoons \tfrac{1}{2}H_2 \qquad (7)$$

Usually, the first zinc layer is stripped off in nitric acid. Thus,

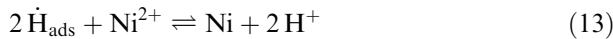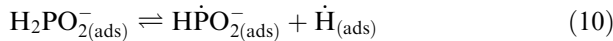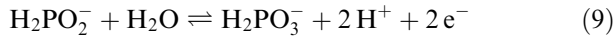$$2\,HNO_3 + Zn \rightleftharpoons Zn(NO_3)_2 + H_2 \uparrow \qquad (8)$$
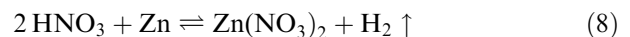
Thereafter, a second zinc immersion is applied before electroless nickel deposition is performed. The second zinc deposit ($\sim 0.15\,\mu$m using a modified alloy zincate solution [22]) is more compact and presents a larger number of fine grains compared to the first layer, inhibiting oxide reformation on the aluminium substrate [19].

3. Hydrogen evolution during the electroless nickel deposition

The electroless nickel deposition from hypophosphite solution involves a complex mechanism which is still a subject of controversy [23, 24], mainly regarding the

oxidation of hypophosphite on the catalytic surface. However, according to the proposed [6, 7, 23] oxidation mechanism (via homolysis or heterolysis of hypophosphite molecule), active hydrogen species like H^+ or $\dot{H}$ are continuously generated and/or consumed in the system. Such reactions include:

$$H_2PO_2^- + H_2O \rightleftharpoons H_2PO_3^- + 2H^+ + 2e^- \tag{9}$$

$$H_2PO_{2(ads)}^- \rightleftharpoons H\dot{P}O_{2(ads)}^- + \dot{H}_{(ads)} \tag{10}$$

$$2H^+ + 2e^- \rightleftharpoons H_2 \uparrow \tag{11}$$

$$2\dot{H}_{ads} \rightleftharpoons H_2 \uparrow \tag{12}$$

$$2\dot{H}_{ads} + Ni^{2+} \rightleftharpoons Ni + 2H^+ \tag{13}$$

As a result, at the catalytic surface/solution interface, part of the active hydrogen species can be discharged and consequently adsorbed on the catalytic surface. As the NiP coating is continuously growing, hydrogen may also become entrapped (absorbed) in the coating. Recombination of hydrogen ions and atoms to H_2, which escape the system, also occurs.

A scheme of the hydrogen evolution at the catalytic surface/solution interface can be represented as in Figure 1.

4. Experimental procedure

4.1. Coating preparation

NiP and NiP–X (X = SiC, Al_2O_3 and B particles) coatings were obtained using an electroless nickel bath for composite coatings with sodium hypophosphite as reducing agent. Unless otherwise specified, the experimental conditions and procedures were as described in reference [25]. Some of the particle characteristics are summarized in Table 1. The bath was operated at
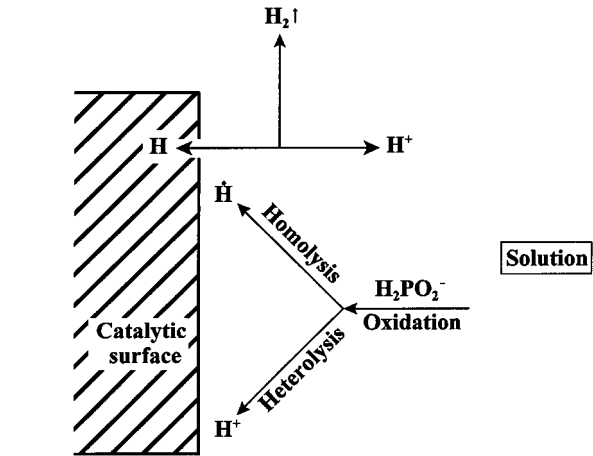

Fig. 1. Schematic representation of hydrogen evolution during electroless nickel plating using hypophosphite as reducing agent.

$87 \pm 2\,^\circ$C over a pH range of 4.6–4.8 (measured at $25\,^\circ$C). Particles were chemically cleaned using 5:1 HCl, rinsed with demineralized water and dried in the oven. All the coatings were deposited on an aluminium 6063-T6 (AlMg 0.5Si) substrate; the ratio surface area/bath volume was between 1 and 1.5 dm^{-1}. To ensure a good deposition of the subsequent layer, prior to the plating, the aluminium substrate was chemically treated using a double immersion zincating sequence [26]. Coating thickness, as measured by optical microscopy, was found to be $41 \pm 3\,\mu$m. Except for NiP–B coating, all the particle concentrations in the layers were determined gravimetrically (Table 1) using nitric acid as stripping agent.

4.2. Hydrogen analysis

The amount of hydrogen in the reinforcement particles, substrate and (as-)deposited plates was measured by the solid extraction method using a Ströhlein H-mat 251 hydrogen gas analyser. The analyser can determine the change in the conductivity of a carrier gas (Ar 99.9999%

Table 1. Main particle characteristics and particle concentration in layers

Particle type	Particle shape	Specific surface area /m^2 g^{-1} [25]	Particle concentration in layer	
			/wt %	/vol %
SiC	irregular	3.7	5.3 ± 0.4	12.4 ± 0.8
Al$_2$O$_3$–I	irregular	3.2	8.4 ± 0.7	15.7 ± 1.3
Al$_2$O$_3$–S	spherical	0.7	9.7 ± 0.8	18.0 ± 1.4
Saffil δ-Al$_2$O$_3$	fibre (F)	18.1	5.4 ± 1.1	10.4 ± 2.0
Boron*	irregular	11.0	1.3 ± 0.04	4.4 ± 0.2

*Particle concentration in NiP–B coating was determined by ICP–OES (inductive coupled plasma optical emission spectrometry) as partial dissolution of boron particles in nitric acid was observed.

was used in this study) due to the presence of hydrogen. The analysis sequence is controlled by a microprocessor. First, the sample is weighed, placed in the oven in an open quartz tube, and then transferred to the heating zone, at 570 °C. The time lapse of each measurement was around 20 min. Hydrogen content was calculated by the microprocessor and displayed in ppm by weight. Reported values represent the average of two determinations for (as-)deposited plates and the average and standard deviations of three determinations for particles.

4.3. Heat treatment

In order to investigate hydrogen release from NiP and NiP–X coatings with temperature, heat treatments at: 130, 160 and 190 °C for 1.5 h each were performed using a Heraeus RL 200 furnace with air recirculation.

5. Results and discussion

Hydrogen content in native aluminium substrate, aluminium substrate after second zincating and as-deposited coatings is presented in Table 2.

5.1. Hydrogen in substrate

The native substrate is an aluminium–magnesium–silicon alloy, 6063-T6 (solution heat treated and artificially

aged), which contains very fine, needle shaped $\beta'' - Mg_2Si$ precipitates along $\langle 100 \rangle$, directions in the aluminium matrix [27]. Hydrogen concentration determined in the native substrate (0.25 ppm) is above the hydrogen solubility limit in solid aluminium (0.035 ppm) and originates from (i) hydrogen present in bulk aluminium, and (ii) water adsorbed on the aluminium surface which is converted into hydrogen during the analysis, according to Reaction 1.

As mentioned earlier, good adhesion between electroless nickel deposit and substrate is obtained if a cleaning and zincating process is applied in order to remove and prevent reformation of the Al_2O_3 layer on the substrate surface. Accordingly, the Al-6063 substrate was chemically treated as follows: 5 min degreasing at 60 °C, 2 min etching, 1 min first desmutting, 30 s first zincating, 30 s second desmutting and 15 s second zincating. As a consequence of the reactions involved in the pretreatment steps (Reactions 2–8), hydrogen content increased to 0.36 ppm after the second zincating.

5.2. Hydrogen in the reinforcement particles

In general, hydrogen present in particles is the result of covalent bonds/compounds (e.g.,─OH, hydrides) formation and water adsorption during their processing and storage.

To estimate the contribution of codeposited particles to the amount of hydrogen in the composite coatings, the hydrogen content of the particles was determined at the same temperature (Table 3). From the alumina particles, Saffil δ-Al_2O_3 fibres and Al_2O_3–I contained comparable amounts of hydrogen (1.74 ± 0.23 ppm and 1.52 ± 0.27 ppm, respectively) which are higher than in the Al_2O_3–S (0.57 ± 0.2 ppm). These differences can be explained taking into account their specific surface area (Table 1). A low specific surface area of Al_2O_3–S (0.7 m^2 g^{-1}) leads to a smaller amount of adsorbed water. As reported previously [25], the alumina fibres have a large specific surface area (18.1 m^2 g^{-1}). The nitrogen adsorption/desorption isotherms of fibres (Figure 2) showed significant hysteresis indicating a microporous structure, capable of adsorbing more

Table 2. Hydrogen content in the Al-6063 substrate and as-deposited coatings

Sample	Hydrogen content/ppm	
	Values	Average
Al-6063 initial	0.24	0.25
	0.25	
Al-6063 2nd zincating	0.40	0.36
	0.31	
NiP	1.81	1.74
	1.66	
NiP–SiC	1.93	1.98
	2.03	
NiP–Al$_2$O$_3$–I	2.14	2.07
	1.99	
NiP–Al$_2$O$_3$–S	1.90	2.00
	2.10	
NiP–Saffil δ-Al$_2$O$_3$	5.79	5.61
	5.43	
NiP–B	5.47	5.28
	5.09	

Table 3. Hydrogen content in particles

Particle type	Hydrogen content/ppm
SiC	3.23 ± 0.42
Al$_2$O$_3$–I	1.52 ± 0.27
Al$_2$O$_3$–S	0.57 ± 0.20
Saffil δ-Al$_2$O$_3$	1.74 ± 0.23
Boron	1773 ± 18

water. On the other hand, the existence of water as water of composition (i.e., either as water of crystallization or as hydroxyl groups) may also contribute to the determined hydrogen level.

SiC particles exhibited a higher hydrogen content (3.23 ± 0.42 ppm) compared to alumina particles. Due to their hydrophobic nature, SiC particles may adsorb less water compared to alumina particles. In this case, the water of composition is probably the main source of hydrogen.

The highest amount of hydrogen found in boron powder (1773 ± 18 ppm) must have arisen from the high content of adsorbed water (~ 0.5 wt.%), water of composition (BH_2O: ~ 0.2 wt.%) and H_2O_2(~ 1 wt.%) as reported by the supplier (H.C. Starck, Germany).

5.3. Hydrogen in as-deposited coatings

Commercial electroless nickel baths include buffers and wetting agents to maintain the required pH values and respectively, to prevent streaking due to the hydrogen present on the catalytic surface. In spite of these, as can be observed from Table 2, in all the plated samples, hydrogen content increased significantly after deposition (up to ~ 16 times in NiP–Saffil δ-Al_2O_3 and NiP–B coatings). Hydrogen concentration in the composite coatings was found to be higher than in the NiP coating (~ 3 times higher in composite coatings with Saffil δ-Al_2O_3 and B compared to NiP coating) and it is assumed to be the result of particle entrapment. The main sources of hydrogen in coatings are as follows: (i) hydrogen absorbed in NiP matrix during plating, (ii) hydrogen and water adsorbed/bound on particles surface and their subsequent entrapment in the layer, and
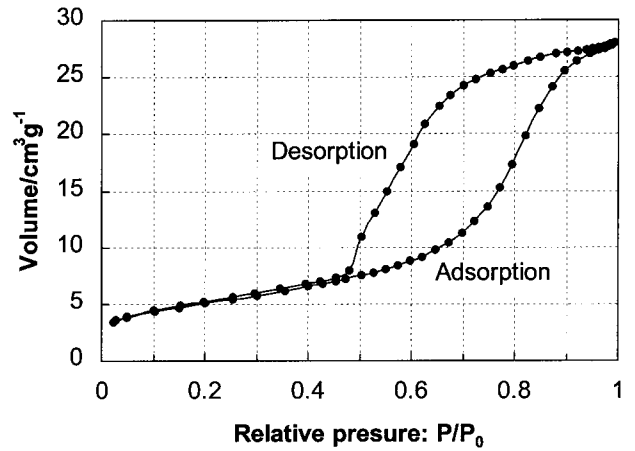

Fig. 2. Adsorption/desorption isotherms of Saffil δ-Al_2O_3 fibres.

(iii) preexistent hydrogen in particles. Composite coatings like NiP–Saffil δ-Al_2O_3 and NiP–B showed a remarkable increase in the hydrogen content compared to the others because both, Saffil δ-Al_2O_3 and boron particles have a high specific surface area, and can adsorb/bind more hydrogen, water or other additives containing hydrogen from electroless nickel bath. For NiP–B coatings, a major contribution is expected from the hydrogen present in boron particles themselves, despite the lower particle concentration found in the layer.

5.4. Hydrogen release from coatings by heat treatment

Hydrogen evolution of NiP and NiP–X coatings with heat treatment temperature is presented in Figure 3. The heat treatments were performed in an air recirculated
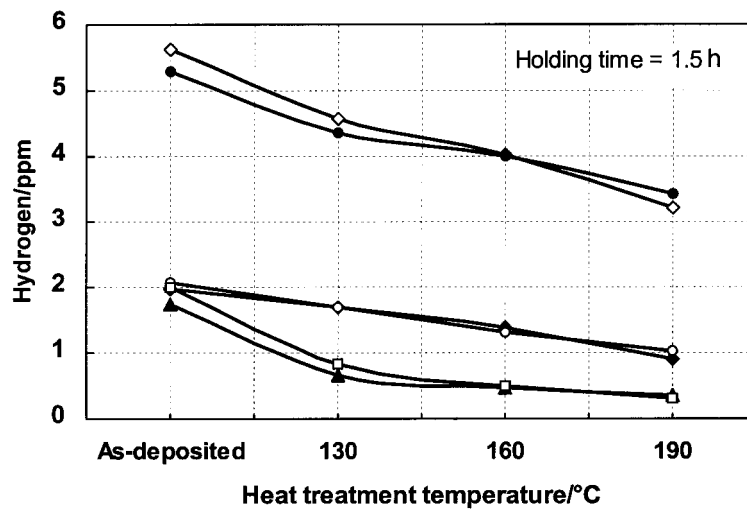

Fig. 3. Coating hydrogen evolution against heat treatment temperature. Key: (▲) NiP; (◆) NiP–SiC; (○) NiP–Al$_2$O$_3$–I; (□) NiP–Al$_2$O$_3$–S; (◇) NiP–Al$_2$O$_3$–F; (●) NiP–B.

oven, at three different temperatures, (i.e., 130, 160, and 190 °C) for a duration of 1.5 h each. As expected, hydrogen content in both the composite coatings and the NiP layer decreased continuously with heat treatment temperature. However, the removal efficiency after the heat treatment at 190 °C/1.5 h varied in the NiP layer and NiP composite coatings. The fact that about 80% of hydrogen content could be released from the NiP layer without particles indicates that hydrogen can diffuse relatively easily through the layer matrix and can be efficiently removed by this heat treatment. As far as the NiP–Al$_2$O$_3$–S coating is concerned the result (85% removal efficiency) indicates that Al$_2$O$_3$–S particles have introduced a very low amount of hydrogen in the coating due to both their low hydrogen content and low specific surface area. As a consequence, it is expected that most of the hydrogen released was from the NiP matrix. For all the other composite coatings, hydrogen removal efficiencies were significantly lower (35–54%) and suggest that when hydrogen is introduced through the particles it is more difficult to be released by heat treatment as a more complex mechanism involving gas diffusion through both particles and metal matrix is likely to occur. As the hydrogen content in the composite coatings increases its removal efficiency seems to decrease.

As previously reported [26], the NiP (8.22 wt. % P) deposits have an amorphous structure and crystalline phases are expected to appear above 350 °C. Thus, the heat treatments performed in this study do not affect the structure of the as-deposited coatings while the adhesion between coating and substrate can be improved as a result of hydrogen decrease.

6. Conclusions

The solid extraction method was used to investigate hydrogen evolution in several electroless composite coatings, that is, NiP–X (X = SiC, Al$_2$O$_3$ and boron) deposited on an aluminium substrate (6063-T6). A global view of hydrogen content in all the investigated
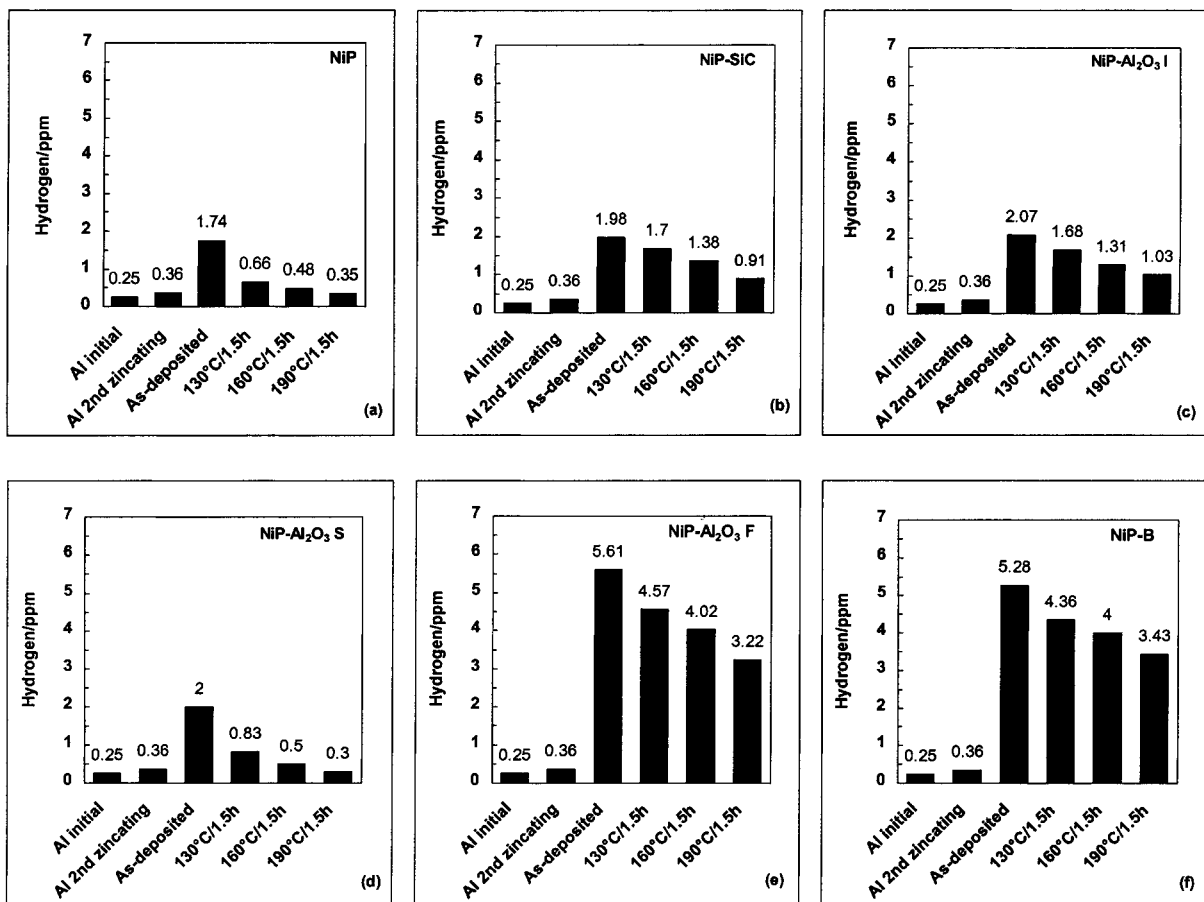

Fig. 4. Amount of hydrogen incorporated during plating and released by heat treatment: (a) NiP; (b) NiP–SiC; (c) NiP–Al$_2$O$_3$–I; (d) NiP–Al$_2$O$_3$–S; (e) NiP–Saffil δ-Al$_2$O$_3$ and (f) NiP–B.

coatings, starting with native substrate and ending with heat treatment at $190\,^{\circ}\mathrm{C}/1.5\,\mathrm{h}$ is presented in Figure 4.

This research confirmed that electroless nickel deposition can introduce hydrogen in as-deposited coatings, as it is involved in the plating mechanism [9, 10, 23]. Hydrogen content in all the as-deposited coatings was significantly higher (i.e., 7–22 times) than in the aluminium substrate.

All the composite coatings presented higher hydrogen content compared to the NiP coating. In general, the amount of hydrogen introduced in the composite coatings could be correlated with the adsorption capacity and the affinity of particles towards water or hydrogen itself.

By heat treatment at different temperatures hydrogen could be released to certain extents from the as-deposited coatings. Hydrogen removal efficiency increased with heat treatment temperature. Heat treatment at $190\,^{\circ}\mathrm{C}/1.5\,\mathrm{h}$ can be considered very efficient for NiP and NiP–Al_2O_3–S coatings since their hydrogen content could be reduced by $\sim$80%. However, for all the other composite coatings a much lower removal efficiency (35–54%) was obtained as a consequence of high hydrogen content introduced through the particles.

Acknowledgements

References

1. J.J. DeLuccia, In: L. Raymond (ed.), *Hydrogen Embrittlement: Prevention and Control*, ASTM, Philadelphia, (1988) p. 17.
2. M. Zamanzadeh, A. Allam, C. Kato, B. Ateya and H.W. Pickering, *J. Electrochem. Soc.* **129** (1982) 284.
3. F.H. Froes, D. Eliezer and H.G. Nelson, In: A.W. Thompson and N.R. Moody (eds), *Hydrogen Effects in Materials*, Minerals, Metals & Materials Society, (1996) p. 719.
4. D. Barker, *Trans. Inst. Metal Finish.* **71** (1993) 121.
5. P. Vanýsek, In: D.R. Lide (ed.), *CRC Handbook of Chemistry and Physics*, 76th edn, CRC Press, (1995) p. 8–21.
6. A. Brenner and G.E. Riddell, *J. Res. Natl. Bur. Stand.* **37** (1946) 31.
7. J.E.A.M. van den Meerakker, *J. Appl. Electrochem.* **11** (1981) 395.
8. W.D. Fields, R.N. Duncan, J.R. Zickgraf and The ASM Committee on Electroless Nickel Plating, In: *Metals Handbook*, 9th edn, vol. 5, ASM, Metals Park, OH, (1982) p. 219.
9. W. Riedel, *Electroless Nickel Plating*, ASM International, Metals Park, OH, and Finishing Publications Ltd., Stevenage, UK, (1991) p. 17.
10. A. Szasz, D.J. Fabian, Z. Paal and J. Kojnok, *J. Non-Cryst. Solids* **103** (1988) 21.
11. P. Shewmon, *Diffusion in Solids*, 2nd edn, Minerals, Metals & Materials Society, Pennsylvania, (1989) p. 122.
12. L.F. Mondolfo, *Aluminium Alloys: Structure and Properties*, Butterworths, London, (1976) p. 295.
13. P.D. Hess, *J. Metals* **25** (10), (1973) 46.
14. L. Kowalski, B.M. Korevaar and J. Duszczyk, *J. Mater. Sci.* **27** (1992) 2770.
15. J.R. Davis and Associates (eds), *Aluminium and Aluminium Alloys*, ASM International, Materials Park, OH, (1993) p. 42.
16. J.H. ter Haar and J. Duszczyk, *J. Mater. Sci.* **28** (1993) 3103.
17. J.W. Golby and J.K. Dennis, *Surf. Technol.* **12** (1981) 141.
18. D.S. Lashmore, *Plat. Surf. Finish.* **67** (1980) 37.
19. S. Wernick, R. Pinner and P.G. Sheasby (eds), *The Surface Treatment and Finishing of Aluminium and its Alloys*, 5th edn, vol. 2, chapter 14, ASM International, Metals Park, OH and Finishing Publications Ltd., Teddington, UK, (1987) p. 1024.
20. K.P. Thurlow, *Trans. Inst. Metal Finish.* **67** (1989) 82.
21. B. Chatterjee and R.W. Thomas, *Trans. Inst. Metal Finish.* **54** (1976) 17.
22. F.J. Monteiro and D.H. Ross, *Trans. Inst. Metal Finish.* **62** (1985) 155.
23. J. Dugasz and A. Szasz, *Surf. Coat. Technol.* **58** (1993) 57.
24. L.M. Abrantes and J.P. Correia, *J. Electrochem. Soc.* **141** (1994) 2356.
25. I. Apachitei, J. Duszczyk, L. Katgerman and P.J.B. Overkamp, *Scripta Mater.* **38** (1998) 1383.
26. I. Apachitei, J. Duszczyk, L. Katgerman and P.J.B. Overkamp, *Scripta Mater.* **38** (1998) 1347.
27. Y. Murakami, In: R.W. Cahn, P. Haasen and E.J. Kramer (eds), vol. 8, *Materials Science and Technology: A Comprehensive Treatment, Structure and Properties of Nonferrous Alloys*, K.H. Matucha (vol. ed.), VCH, Weinheim, Germany (1996) p. 248.